Quantum Simulations on a Quantum Computer

S. Somaroo,[1] C. H. Tseng,[1,2] T. F. Havel,[1] R. Laflamme,[3] and D. G. Cory[4,*]

[1]*BCMP Harvard Medical School, 240 Longwood Avenue, Boston, Massachusetts 02115*

[2]*Harvard-Smithsonian Center for Astrophysics, 60 Garden Street, Cambridge, Massachusetts 02138*

[3]*Los Alamos National Laboratory, Los Alamos, New Mexico 87455*

[4]*Department of Nuclear Engineering, Massachusetts Institute of Technology, Cambridge, Massachusetts 02139*

(Received 6 January 1999)

We present a general scheme for performing a simulation of the dynamics of one quantum system using another. This scheme is used to experimentally simulate the dynamics of truncated quantum harmonic and anharmonic oscillators using nuclear magnetic resonance. We believe this to be the first explicit physical realization of such a simulation. [S0031-9007(99)09457-0]

PACS numbers: 03.67.–a, 76.60.–k

In 1982, Feynman proposed that a quantum system would be more efficiently simulated by a computer based on the principles of quantum mechanics rather than by one based on classical mechanics [1]. Recently, it has been pointed out that it should be possible to efficiently approximate any desired Hamiltonian within the standard model of a quantum computer by a sparsely coupled array of two-state systems [2–4]. Many of the concepts of quantum simulation are implicit in the average Hamiltonian theory developed by Waugh and colleagues to design NMR pulse sequences which implement a specific desired effective NMR Hamiltonian [5]. Here we show the first explicit simulation of one quantum system by another, namely, the simulation of the kinematics and dynamics of a truncated quantum oscillator by an NMR quantum information processor [6,7]. Quantum simulations are shown for both an undriven harmonic oscillator and a driven anharmonic oscillator.

A general scheme for quantum simulation is summarized by the following diagram:

$$\begin{array}{ccc} \text{Simulated } (S) & & \text{Physical } (P) \\ |s\rangle & \xrightarrow{\phi} & |p\rangle \\ {\scriptstyle U=e^{-i\mathcal{H}_s T/\hbar}}\downarrow & & \downarrow {\scriptstyle V_T} \\ |s(T)\rangle & \xleftarrow{\phi^{-1}} & |p_T\rangle . \end{array}$$

The object is to simulate the effect of the evolution $|s\rangle \xrightarrow{U} |s(T)\rangle$ using the physical system P. To do this, S is related to P by an invertible map ϕ which determines a correspondence between all of the operators and states of S and P. In particular, the propagator U maps to $V_T = \phi^{-1} U \phi$. The challenge is to implement V_T using propagators V_i arising from the available external interactions with intervening periods of natural evolution $e^{-i\mathcal{H}_p^0 t/\hbar}$ in P so that $V_T = \Pi_i e^{-i\mathcal{H}_p^0 t_i(T)} V_i$. If a sufficient class of simple operations (logic gates) are implementable in the physical system, the universal computation theorem [8–10] guarantees that any operator (in particular V_T) can be composed of natural evolutions in P and external interactions. For unitary maps ϕ, we may write $V_T = e^{-i\overline{\mathcal{H}}_p T/\hbar}$, where $\overline{\mathcal{H}}_p \equiv \phi^{-1}\mathcal{H}_s\phi$ can be identified with the average Hamiltonian of Waugh. After $|p\rangle \xrightarrow{V_T} |p_T\rangle$, the final map ϕ^{-1} takes $|p_T\rangle \rightarrow |s(T)\rangle$, thereby effecting the simulation $|s\rangle \rightarrow |s(T)\rangle$. Note that $\mathcal{H}_s(T)$ can be a time dependent Hamiltonian and that T is viewed as a parameter when mapped to P. This implies that the physical times $t_i(T)$ are parametrized by the simulated time T.

Liquid state NMR quantum computers are well suited for quantum simulations because they have long spin relaxation times (T_1 and T_2) as well as the flexibility of using a variety of molecular samples. In particular, the coupling between the nuclear spins, usually dominated by the "scalar" coupling (J), may be reduced at will by means of radio frequency pulses. Typically spin-1/2 nuclei are used. Thus, the kinematics of any 2^N level quantum system could be simulated using a given N-spin molecule.

We chose to simulate a quantum harmonic oscillator (QHO) with a 4-level, 2-spin system P being the two proton nuclear spins in 2,3-dibromothiophene. The Hamiltonian of a QHO is $\mathcal{H}_{\mathrm{QHO}} \equiv \hbar\Omega(\hat{N} + \frac{1}{2}) = \sum_n \hbar\Omega(n + \frac{1}{2})|n\rangle\langle n|$, where Ω is the oscillator frequency and $|n\rangle$ are the orthonormal eigenstates of the number operator $\hat{N}$. Since the nuclear spin eigenstate space is finite dimensional (4 levels, in this case), only a truncated version of the infinite dimensional oscillator was simulated. However, as noted above, for N spins, there are 2^N levels. A convenient unitary mapping, ϕ, between the energy eigenstates of the QHO and a 2-spin system is

$$\begin{aligned} |n=0\rangle &\longleftrightarrow |\uparrow\rangle|\uparrow\rangle \equiv |\uparrow\uparrow\rangle, \\ |n=1\rangle &\longleftrightarrow |\uparrow\rangle|\downarrow\rangle \equiv |\uparrow\downarrow\rangle, \\ |n=2\rangle &\longleftrightarrow |\downarrow\rangle|\downarrow\rangle \equiv |\downarrow\downarrow\rangle, \\ |n=3\rangle &\longleftrightarrow |\downarrow\rangle|\uparrow\rangle \equiv |\downarrow\uparrow\rangle . \end{aligned} \tag{1}$$

While any number of mappings would suffice, this mapping is convenient since $\Delta n = \pm 1$ corresponds to allowed transitions in P. This mapping generalizes to a Gray code. Also note that the spin basis, permuted under ϕ, is now not in order of increasing energy in P.

When truncated, $e^{-i\mathcal{H}_{\mathrm{QHO}}T/\hbar}$ is mapped onto the 2-spin system as follows:

$$U = e^{-i\mathcal{H}_s T/\hbar} \equiv \exp[-i(\tfrac{1}{2}|0\rangle\langle 0| + \tfrac{3}{2}|1\rangle\langle 1| + \tfrac{5}{2}|2\rangle\langle 2| + \tfrac{7}{2}|3\rangle\langle 3|)\Omega T],$$
$$\xrightarrow{\phi} V_T = e^{-i\overline{\mathcal{H}}_p T/\hbar} \equiv \exp[-i(\tfrac{1}{2}|\uparrow\uparrow\rangle\langle\uparrow\uparrow| + \tfrac{3}{2}|\uparrow\downarrow\rangle\langle\uparrow\downarrow| + \tfrac{5}{2}|\downarrow\downarrow\rangle\langle\downarrow\downarrow| + \tfrac{7}{2}|\downarrow\uparrow\rangle\langle\downarrow\uparrow|)\Omega T].$$

Using the Pauli matrices $\{\sigma_x, \sigma_y, \sigma_z\}$ as a basis for the 2-spin density matrices [11], we may write

$$V_T = e^{-i\overline{\mathcal{H}}_p T/\hbar} = \exp[i\{\sigma_z^2(1 + \tfrac{1}{2}\sigma_z^1) - 2\}\Omega T]. \quad (2)$$

Implementing the operator (2) on the 2-spin system thus constitutes a simulation of the truncated QHO. This is easily done by making various refocusing adjustments to the physical 2-spin propagator $e^{-i\mathcal{H}_p^0 t_i/\hbar}$, obtained from the natural Hamiltonian $\mathcal{H}_p^0 \equiv \frac{\hbar}{2}[(\omega_1 - \omega_0)\sigma_z^1 + (\omega_2 - \omega_0)\sigma_z^2 + \pi J\sigma_z^1\sigma_z^2]$, where $\omega_{1,2}/2\pi$ are the resonance frequencies of spins 1 and 2, $(\omega_2 - \omega_1)/2\pi = 226$ Hz, $\omega_0/2\pi$ is the spectrometer frequency (~400 MHz), and J is a scalar coupling strength (5.7 Hz). The following on-resonance ($\omega_0 = \omega_1$) pulse sequence implements V_T for the simulated period ΩT:

$$V_T = [\pi]_y^{1+2} - [\tau_1/2] - [\pi]_y^{1+2} - [\tau_1/2 + \tau_2]. \quad (3)$$

The symbol $[\pi]_y^{1+2}$ represents a π angle radio frequency pulse, oriented along the y direction, on spins 1 and 2 (corresponding to the V_i), and $[\tau]$ represents a delay during which the 2-spin propagator $e^{-i\mathcal{H}_p^0\tau/\hbar}$ acts. The time intervals are given by $\tau_1 = \Omega T[1/(\pi J) - 2/(\omega_2 - \omega_1)]$ and $\tau_2 = 2\Omega T/(\omega_2 - \omega_1)$.

The experimental procedure is illustrated using $|s\rangle = |0\rangle + i|2\rangle$ as follows:

$$|s\rangle = |0\rangle + i|2\rangle \Leftrightarrow |p\rangle\langle p| = \begin{pmatrix} 1 & \boxed{0\ 0} & -i \\ \boxed{0\\0} & 0\ 0 & \boxed{0\\0} \\ i & \boxed{0\ 0} & 1 \end{pmatrix} \overset{V_T}{\Rightarrow} |p_T\rangle\langle p_T| = \begin{pmatrix} 1 & \boxed{0\ 0} & -ie^{i2\Omega T} \\ \boxed{0\\0} & 0\ 0 & \boxed{0\\0} \\ ie^{i2\Omega T} & \boxed{0\ 0} & 1 \end{pmatrix}$$

$$\overset{\text{Read } [\frac{\pi}{2}]_y^1}{\Rightarrow} \begin{pmatrix} 1 & \boxed{1\ ie^{i2\Omega T}} & -ie^{i2\Omega T} \\ \boxed{1\\-ie^{-i2\Omega T}} & 1\ \ ie^{i2\Omega T} & \boxed{-ie^{i2\Omega T}\\-1} \\ ie^{i2\Omega T} & \boxed{ie^{-i2\Omega T}\ -1} & 1 \end{pmatrix}$$

The initial state $|p\rangle = |\uparrow\uparrow\rangle + i|\downarrow\downarrow\rangle \leftrightarrow |s\rangle$, is easily prepared from the (pseudopure [6]) state $|\uparrow\uparrow\rangle$. This in turn is produced from the thermal equilibrium state of 2,3-dibromothiophene by the sequence $[\pi/4]_x^{1+2} - [1/4J] - [\pi]_y^{1+2} - [1/4J] - [-5\pi/6]_y^{1+2} - [G]$, where the magnetic field gradient $[G]$ destroys off-diagonal terms in the density matrix. The sequence (3) for V_T then leads to $|p_T\rangle\langle p_T|$. Since the simulated system should evolve coherently according to the difference in energy levels of the various superpositions, $|p_T\rangle\langle p_T|$ above expresses a $2\Omega T$ dependence. Nuclear magnetic resonance experiments are sensitive only to transverse dipolar magnetization, corresponding to the boxed components in the density matrices above. Thus a final read pulse is needed to rotate the $e^{\pm i2\Omega T}$ elements into view. The result manifests itself as a $2\Omega T$ oscillation of the spectral peak heights as a function of the indirect dimension T.

The dynamics of the truncated QHO states $|0\rangle$, $(|0\rangle + i|2\rangle)$, and $(|0\rangle + |1\rangle + |2\rangle + |3\rangle)$ were simulated. Eigenstates such as $|0\rangle$ do not evolve, as the simulation in Fig. 1(*a*) shows. Figure 1(*b*) shows the $2\Omega T$ oscillations discussed above for $|0\rangle + i|2\rangle$. In both Figs. 1(*a*) and 1(*b*), $[\pi/2]_y$ read pulses were used. For $|s\rangle = |0\rangle + |1\rangle + |2\rangle + |3\rangle$, mixtures of ΩT and $3\Omega T$ oscillations can be observed in the spectra. For example, the operator $|0\rangle\langle 1|$ corresponds to $|\uparrow\uparrow\rangle\langle\uparrow\downarrow|$ which is a transition of spin 2. Thus the amplitude of the spin-2 peak will oscillate at ΩT. In Fig. 1(*c*), ΩT peak oscillations (on spin 2) are recorded while Fig. 1(*d*) shows a superposition of ΩT and $3\Omega T$ (on spin 1). Since the 2-spin system (P) has no natural triple quantum coherences, the latter coherence is entirely simulated. For Figs. 1(*c*) and 1(*d*), read pulses were not required.

In general, scaling the above to include more levels will depend on the various couplings between the added spins. For larger spin systems certain couplings are small and therefore severely limit the time scale of the experiment. For the truncated QHO, however, an effective Hamiltonian that is free of all couplings results from mapping the energy eigenstate $|k\rangle$ to the spin eigenstate corresponding to the binary representation of k, in contrast to the Gray coding:

$$\overline{\mathcal{H}}_p = \tfrac{1}{2}\hbar\Omega(2^n - [\sigma_z^1 + 2\sigma_z^2 + 2^2\sigma_z^3 + \cdots + 2^{n-1}\sigma_z^n]).$$

This may be implemented by removing all scalar couplings and scaling all chemical shifts, for instance by methods analogous to "chemical shift concertina" sequences introduced by Waugh [12].

The Hamiltonian for an anharmonic oscillator, $\mathcal{H}_{\mathrm{AHO}} = \hbar\Omega[(\hat{N} + \frac{1}{2}) + \mu(\hat{N} + \frac{1}{2})^2]$, where μ is the anharmonicity parameter. The energy difference ΔE_m between the mth and $(m + 1)$st energy level is $\Delta E_m = \hbar\Omega[2\mu(m + 1) + 1]$. Radiation at the frequency $\Delta E_m/h$ will drive a selective transition

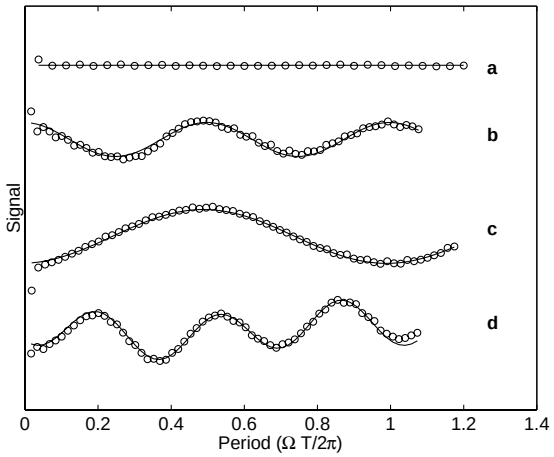

FIG. 1. NMR peak signals from 2,3-dibromothiophene demonstrating a quantum simulation of a truncated harmonic oscillator as implemented by V_T in (3). The various initial states express oscillations according to the energy differences between the eigenstates involved. The solid lines are fits to theoretical expectations. *a*: Evolution of the initial (pseudo-pure) state $|0\rangle$, showing no oscillation. *b*: Evolution of the initial state $|0\rangle + i|2\rangle$, showing 2Ω oscillations. *c*: Evolution of the initial state $|0\rangle + |1\rangle + |2\rangle + |3\rangle$ showing the Ω, and *d*: 3Ω oscillations. (Each trace in *c* and *d* is actually a combination of Ω and 3Ω oscillations.)

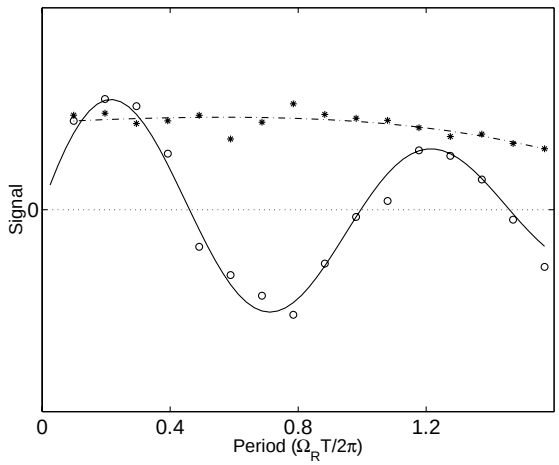

FIG. 2. NMR peak signals from 2,3-dibromothiophene demonstrating a quantum simulation of a driven, truncated anharmonic oscillator as implemented by V_T in (4). When the (0,1) transition is selectively driven, the initial state $|0\rangle$ ($\circ$) undergoes Rabi (Ω_R) oscillations to the $|1\rangle$ state, whereas the $|2\rangle$ state ($*$) does not evolve under the simulated Hamiltonian. The exponential decay due to natural decoherence in P is clear.

between these levels. The Hamiltonian for this selectively driven anharmonic oscillator is $\mathcal{H}_{\mathrm{AHO}} + \frac{1}{2}\hbar\Omega_R(|m\rangle\langle m+1| + |m+1\rangle\langle m|)$, where Ω_R is the Rabi frequency. Using the map (1), the $|0\rangle \leftrightarrow |1\rangle$ driven truncated Hamiltonian in particular maps to

$$\overline{\mathcal{H}}_p \equiv \tfrac{1}{4}\hbar\Omega[\mu\sigma_z^1 - 4(4\mu+1)\sigma_z^2(1+\tfrac{1}{2}\sigma_z^1)] + \tfrac{1}{4}\hbar\Omega_R\sigma_x^1(1+\sigma_z^2).$$

This is implemented on 2,3-dibromothiophene by the following pulse sequence:

$$V_T = [\tau_1/2] - [\pi]_y^1 - [\tau_1/2] - [3\pi/4]_y^1 - [\tau_2] - [\pi/4]_y^1. \quad (4)$$

For $\mu = -2/9$, and $\Omega_R = -2/9\Omega$, the time intervals are determined by $\Omega T/2\pi = 9J\tau_2/(2\sqrt{2}) = (9/2)(m - \tau_1\omega_2/2\pi)$, where m is an integer. The receiver was set at $\omega_0/2\pi = \omega_1/2\pi - J/2$. Note that the map (1) does not map the physical eigenstates to the simulated eigenstates (dressed states) of the driven oscillator, emphasizing that knowledge of the eigenvalues/states of the simulated system is not assumed. Experimental results are shown in Fig. 2.

In these studies, we have considered only unitary evolution and have explored the quantum dynamics for systems without dissipation. The decoherence [13] intrinsic in our physical system (characterized by the longitudinal and transverse magnetization relaxation times T_1 and T_2) limits the time of the experiment. This then limits the number of periods that can be simulated. Since the experimental (t) and simulated (T) time scales need not be identified with each other, this can be interpreted as a restriction either on Ω or on T. In Fig. 2 the visible decay due to T_2 relaxation clearly shows this limitation. While decoherence can be controlled, in principle, by error correction [14–16], it would be difficult to utilize this in the weakly polarized physical system used here. Moreover, thermal equilibrium will not necessarily map to another configuration that is thermal. Decoherence itself may be simulated through specific nonunitary evolution; in NMR, for example, by magnetic field gradients [17].

The aspects available in the simulation: controlled kinematics and dynamics, a driving field, and decoherence, suggest a very general tool with which to study other systems.

This work was supported in part by the U.S. Army Research office under Contract/Grant No. DAAG 55-97-1-0342 from the DARPA Ultrascale Computing Program. R. L. thanks the National Security Agency for support.

*Author to whom correspondence and requests for materials should be addressed.
Email address: dcory@mit.edu

[1] R. Feynman, Int. J. Theor. Phys. **21**, 467 (1982).
[2] S. Lloyd, Science **261**, 1569 (1993).
[3] S. Lloyd, Science **273**, 1073 (1996).
[4] C. Zalka, Proc. R. Soc. London A **454**, 313 (1998).
[5] U. Haeberlen and J. Waugh, Phys. Rev. **175**, 453 (1968).
[6] D. Cory, A. Fahmy, and T. Havel, Proc. Natl. Acad. Sci. U.S.A. **94**, 1634 (1997).
[7] N. Gershenfeld and I. Chuang, Science **275**, 350 (1997).

[8] A. Barenco, C. Bennett, R. Cleve, D. DiVincenzo, N. Margolus, P. Shor, T. Sleator, J. Smolin, and H. Weinfurter, Phys. Rev. A **52**, 3457 (1995).
[9] S. Lloyd, Phys. Rev. Lett. **75**, 4714 (1995).
[10] D. P. DiVincenzo, Phys. Rev. A **51**, 1015 (1995).
[11] S. Somaroo, D. Cory, and T. Havel, Phys. Lett. A **240**, 1 (1998).
[12] J. Ellett and J. S. Waugh, J. Chem. Phys. **51**, 2581 (1969).
[13] W. H. Zurek, Phys. Today **44**, No. 10, 36 (1991).
[14] P. W. Shor, Phys. Rev. A **52**, 2493 (1995).
[15] A. Steane, Proc. R. Soc. London A **452**, 2551 (1996).
[16] E. Knill, R. Laflamme, and W. Zurek, Science **279**, 342 (1998).
[17] D. Cory, M. Price, W. Maas, E. Knill, R. Laflamme, W. Zurek, T. Havel, and S. Somaroo, Phys. Rev. Lett. **81**, 2152 (1998).